Available online at www.sciencedirect.com

ScienceDirect

www.elsevier.com/locate/jes

JES JOURNAL OF ENVIRONMENTAL SCIENCES

www.jesc.ac.cn

Preparation, characterization and performance of poly(*m*-phenylene isophthalamide)/organically modified montmorillonite nanocomposite membranes in removal of perfluorooctane sulfonate

Qin Luo[1,2], *Yanxia Liu*[1], *Guixia Liu*[1,*], *Changwei Zhao*[2,*]

1. *Key Laboratory of Applied Chemistry and Nanotechnology at Universities of Jilin Province, Changchun University of Science and Technology, Changchun 130022, China*
2. *State Key Laboratory of Environmental Aquatic Chemistry, Research Center for Eco-Environmental Sciences, Chinese Academy of Sciences, Beijing 100085, China*

ARTICLE INFO

Article history:
Received 9 April 2015
Revised 22 October 2015
Accepted 23 October 2015
Available online 25 March 2016

Keywords:
Nanofiltration membrane
Organically modified montmorillonite
PFOS removal

ABSTRACT

Nanocomposite membranes containing poly(*m*-phenylene isophthalamide) (PMIA) and organically modified montmorillonite (OMMT) were prepared by a combination of solution dispersion and wet-phase inversion methods, and the effects of OMMT addition on the properties and performance of fabricated nanofiltration membranes were investigated. The membranes were characterized by contact angle measurements, scanning electron microscopy (SEM), atomic force microscopy (AFM), thermogravimetric analysis, and zeta potential. The performance of the membranes was elucidated by the removal of perfluorooctane sulfonate (PFOS) at neutral pH. Increasing OMMT concentration improved the thermal stability and hydrophilicity of the membranes. The permeation and rejection of PFOS were significantly improved. The performance of fabricated nanofiltration membranes in removal of PFOS varied depending on the solute and membrane properties as well as solution conditions. Finally, a comparison between fabricated membranes and a commercial NF membrane (ESNA1-K1, Hydecanme) proved that the OMMT addition is a convenient procedure for producing nanocomposite membranes with superior properties and performance.

© 2016 The Research Center for Eco-Environmental Sciences, Chinese Academy of Sciences. Published by Elsevier B.V.

Introduction

In recent years, there has been increasing concern about the global contamination of water environments caused by the widespread use of perfluorinated compounds (PFCs). Potassium perfluorooctane sulfonate (PFOS) is a typical PFC and has a range of applications, *e.g.*, in surfactants, fire retardants, lubricants, and polymer additives (Moody et al., 2001; Giesy and Kannan, 2001; Moody and Field, 2000). Although PFOS was listed as a persistent organic pollutant (Tang et al., 2006), its use is still allowed in some industries, *e.g.*, chrome plating in China. It has been reported that the concentrations of PFOS in surface waters near industrial zones were as high as 5.7 μg/L (Rattanaoudom et al., 2012). It is important to remove PFOS from such point sources before discharge into the environment. However, PFOS is very stable, and it is difficult to decompose in ambient environments using conventional techniques, such as biological degradation, oxidation, and reduction (Vecitis et al., 2009). Conventional

* *Corresponding authors.* E-mail address: liuguixia22@163.com (Guixia Liu).

http://dx.doi.org/10.1016/j.jes.2015.10.032
1001-0742/© 2016 The Research Center for Eco-Environmental Sciences, Chinese Academy of Sciences. Published by Elsevier B.V.

treatment methods are inadequate and may even produce toxic byproducts. The performance required of removal processes is also becoming increasingly stringent. Membranes provide an alternative method for effectively removing PFOS from wastewater; they are cheap, simple to operate, and use less chemicals (Baker, 2004).

Nanofiltration membranes are one of the most important types of membrane for the removal of multivalent ions and organic compounds (100–1000 Da), especially persistent organic pollutants, from water and wastewater sources. Research on improving nanofiltration properties has focused on modification of membrane materials, in order to increase the strength, heat resistance and so forth. Among various inorganic fillers, *e.g.*, zeolites (Gevers et al., 2005), inorganic compounds (Rajesh et al., 2012; Fang and Duranceau, 2013; Romanos et al., 2012; Pourjafar et al., 2012; Namvar-Mahboub and Pakizeh, 2013; Gholami et al., 2014; Chen et al., 2014), and ceramic oxides (Schmidt et al., 2014; Zhang et al., 2014; Pages et al., 2013), layered silicates are of particular interest, because they can be dispersed in polymeric matrices at the nanoscale. The most-used clays in polymer-clay nanocomposites (PCNs) are those containing smectite clay minerals, particularly organomontmorillonite (OMMT). OMMT is a hydrophilic clay, and its addition at low contents (<10 wt.%) can be useful for producing PCNs with improved properties, and for enhancing the hydrophilicity of the material (Rajesh et al., 2012; Gevers et al., 2005; Schafer et al., 2004; Anadão et al., 2010).

Despite nanocomposite membranes' potential for application in the field of nanofiltration, only a few studies have been devoted to these membranes (Anadão et al., 2010; Monticelli et al., 2007). Poly(*m*-phenylene isophthalamide) (PMIA) is widely used in membranes for various applications (Cheng et al., 2000; Wang et al., 2013; Ren et al., 2010; Yu et al., 2013). In this work, we prepared and characterized PMIA-based nanocomposite membranes containing various concentrations of commercially available OMMT, using a combination of solution dispersion and wet-phase inversion methods. The performance of fabricated membranes was evaluated in terms of the permeation and rejection of solutions containing the selected perfluorooctane sulfonate (PFOS) under different solution conditions. Finally, the ability of these nanocomposite membranes in the removal of PFOS was compared with a commercial nanofiltration membrane, ESNA1-K1.

1. Experimental

1.1. Materials

Fibrous PMIA was obtained from the Yantai Spandex Co., Ltd. (China); its chemical structure is shown in Fig. 1. The polymer

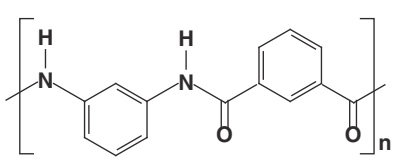

Fig. 1 – Chemical structure of poly(m-phenylene isophthalamide.

was dried for at least 5 hr at 80°C and then used to prepare a polymer solution. Analytical grade *N*, *N′*-dimethylacetamide (DMAc) and LiCl, used as the solvent and cosolvent, respectively, were purchased from the Tianjin Fuchen Chemicals Reagent Factory (China). OMMT clays were purchased from the Beijing Eastwest Specialty Chemicals Co.; schematic drawings are shown in Fig. 2. PFOS (99%) was purchased from AccuStandard, Inc. (USA). A commercial composite polyamide nanofiltration membrane, ESNA1-K1, was kindly supplied by Hydecanme, as a flat sheet. Each experiment was carried out twice and double-distilled water was used in all the experiments.

1.2. Feed

Nanofiltration was carried out with a solution containing PFOS with a concentration of 100 μg/L and at solution pH value of 7.0. Due to their pK_a, perfluorooctane sulfonate (PFOS) molecules are ionized and therefore negatively charged at both neutral and acid solution pH values.

1.3. Preparation of pristine PMIA membrane

A casting solution containing PMIA (20 wt.%) dissolved in DMAc was prepared by stirring for 8 hr at 5.0 Hz (300 r/min) and 50°C. The solution was cast by spreading on a glass plate substrate, using a laboratory-made casting knife, at a thickness of 250 μm. The substrate then was moved to a non-solvent (water) bath for immersion precipitation at room temperature. After primary phase separation and formation of the membrane, it was stored in water for 24 hr to guarantee complete phase separation. This allowed the water-soluble components in the membrane to leach out. The rejection of NaCl and $MgSO_4$ by the PMIA membrane were respectively about 27% and 48%, with a feed concentration of 500 mg/L under 5.5×10^5 Pa. According to the parameters provided for the commercial NF membrane, under the same conditions, the rejection values of the commercial membrane were greater than 92%.

1.4. Preparation of nanocomposite membranes

Nanocomposite membranes were prepared using a combination of wet-phase inversion and solution dispersion techniques. Dispersions with various OMMT contents (0.5%–5%) and 20 wt.% PMIA in DMAc were prepared under vigorous mechanical stirring for 8 hr at 50°C. First, one-quarter of the 20 wt.% PMIA was added, and after solubilization, one-quarter of the total amount of OMMT was added. This procedure was continued until both additions were complete, as previously reported by Anadão et al. The casting and immersion of the nanocomposite membranes were performed using the same method as for the pristine PMIA membrane.

1.5. Membrane characterization

The surface morphologies and thicknesses of the synthesized membranes were examined using scanning electron microscopy (SEM; SU8000, HITACHI) and atomic force microscopy (AFM; Digital Instruments, USA). The arithmetic average (R_a) roughness of the membranes was estimated from topographic images of area 5 μm × 5 μm. The static water contact angles of the

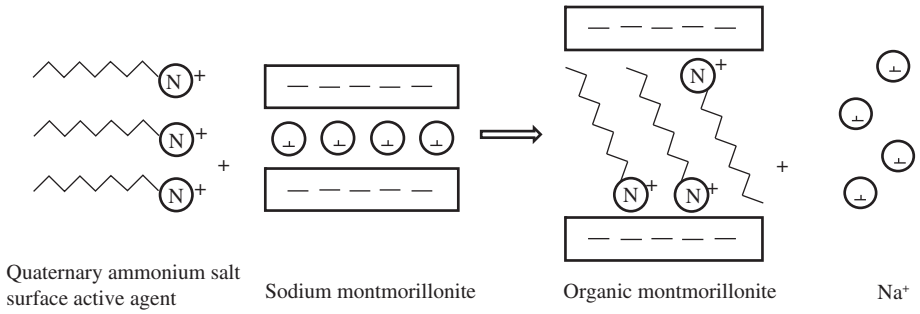

Fig. 2 – Schematic drawings of montmorillonite in the presence of organic cations.

membrane surfaces were measured at room temperature using a goniometer (NRL CA Goniometer, Rame-Hart, Inc.) equipped with a video-capturing apparatus. The average contact angle was determined from eight measurements for each sample. The zeta potential was measured in a background aqueous solution of KI (1 mol/L) containing mobility-monitoring particles. A plate sample cell was used for all membrane samples. Thermogravimetric analysis (TGA; PL-TGA, UK) was performed in the range of 40–750°C in an argon flow of 50 mL/min, at a heating rate of 10°C/min, with a sample mass of about 5 mg.

1.6. *Membrane performance measurements*

The prepared membranes were cut to the size needed for fixing in the nanofiltration kit and initially pressurized with distilled water at 10×10^5 Pa (145 psi) for 2 hr in order to ensure a stable flux. Subsequently, the membranes were subjected to the solute separation experiments whereby different solutions, containing PFOS as well as co-existing anions and Pb^{2+}, were passed through the membrane shell side. The permeation fluxes (*F*) of the membranes can be calculated as:

$$F = \frac{J}{S \times t} \quad (1)$$

where, *F* (L/(m^2·hr)) is the permeation flux of the membrane, *J* (L) is the total volume of permeate during the experiment, *S* (m^2) is the membrane effective area, and *t* (hr) denotes the operating time. The solute rejection was calculated as:

$$R = \left(1 - \frac{c_p}{c_o}\right) \times 100\% \quad (2)$$

where, c_o and c_p are the feed and permeate concentrations, respectively.

In determination of the rejection of PFOS by nanofiltration membranes, adsorption effects on the membrane surface must be considered to avoid overestimation of the rejection (Fang and Duranceau, 2013). Overestimation is important, particularly for neutral compounds and ionizable compounds under electrostatically neutral conditions. A longer operating time was used to reach the saturated state. The required time for membrane saturation depends on the feed concentration (Zhai et al., 2014; Kimura et al., 2003). A higher feed concentration requires a lower operating time to reach the saturated state (steady-state condition) (Zhai et al., 2014). In this study, permeate samples were collected every hour and the membrane was saturated after 5 hr. The rejection rate was reported for steady-state conditions. PFOS removal experiments were performed using a 100 μg/L PFOS solution. The rejection and permeation of the solutions containing PFOS by PMIA and nanocomposite membranes after operation for around 8 hr under neutral conditions were calculated using Eqs. (1) and (2).

2. Results and discussion

2.1. *Effect of OMMT on the properties of nanocomposite membranes*

In order to investigate the effect of clay on the thermal stability of the nanocomposite membranes, thermogravimetric analysis was performed. The TGA curves related to virgin PMIA and PMIA/OMMT membranes are shown in Fig. 3. With increasing addition of OMMT, the onset and final temperatures of degradation of the clay shifted to higher temperatures. In nanocomposite membranes, the enhancement in the thermal stability can be explained by the barrier properties of the clay mineral layers, which restrict the diffusion of oxygen molecules into the nanocomposites, and also by the complicated effect of these layers being dispersed in the PMIA matrix which delays volatilization (Schafer et al., 2004; Monticelli et al., 2007).

The water contact angles were measured (Fig. 4), which are indicative of the wettability of the prepared membranes. Virgin PMIA membrane had the highest contact angle and the lowest hydrophilicity. The water contact angle decreased significantly with increasing OMMT concentration. The PMIA/OMMT$_{5.0}$ membrane exhibited the lowest water contact angle, indicating the highest hydrophilicity. The significant changes in hydrophilicities of the membranes prepared with OMMT can be ascribed to the fact that the organically modified clay is hydrophilic and carries hydrophilic polar ammonium moieties.

The zeta potential measurement data of virgin PMIA and PMIA/OMMT nanocomposite membranes in neutral solution are tabulated in Fig. 4. The data show a decrease in zeta potential values (negative charge) of the membranes with increasing OMMT concentration. Addition of OMMT to the casting solution reduces the negative charge of the membrane. This is probably because the electrostatic attraction between the ammonium parts of OMMT and negative charges of the membrane surface, which diminishes the negative charge of the membrane surface.

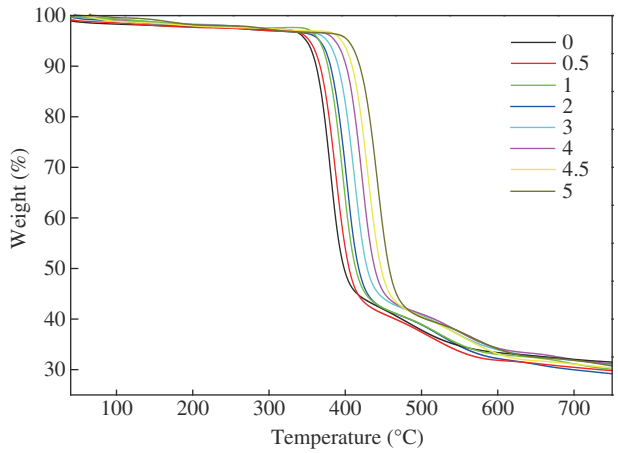

Fig. 3 – TGA curves of pristine PMIA and nanocomposite membranes prepared with various concentrations of OMMT. TGA: Thermogravimetric analysis; PMIA: poly(*m*-phenylene isophthalamide); OMMT: organically modified montmorillonite.

2.2. Effect of OMMT on the morphology of nanocomposite membranes

The performance of membranes strongly depends on the surface, sub-layer morphology, and top layer thickness and compactness (Van der Bruggen et al., 1999; Lu et al., 2006; Nigam et al., 2004). The influence of the concentration of OMMT as the additive on the membrane morphology was investigated using SEM apparatus. There was no obvious difference in the surface morphology of the nanocomposite membranes with different concentrations of OMMT (Fig. 5a).

The variations in the cross-sectional morphology of the membranes were mainly elucidated by SEM (Fig. 5b). The virgin PMIA membrane showed a typical asymmetric structure composed of a thin skin layer and a porous bulk with a finger-like structure. The addition of OMMT to the casting solution resulted in membranes composed of thinner skin layers and a more porous sublayer compared to the virgin PMIA membrane. However, the addition of more than 4 wt.% of OMMT resulted in denser skin layers with increased thickness and sub-layers with lower porosities.

2.3. Effect of OMMT on the performance of nanocomposite membranes in removal of PFOS

The results for the rejection and permeation of a solution containing PFOS molecules using virgin PMIA and nanocomposite membranes, after the operating time of around 8 hr in neutral condition (pH 7.0) and calculated using Eqs. (1) and (2), are depicted in Fig. 6. The operating pressure was 5.5×10^5 Pa (79.75 psi). The rejection was improved with increasing concentration of OMMT. The flux was significantly increased with an increment in OMMT concentration from 0 to 4 wt.%, then it was decreased as the concentration of OMMT reached 5%.

In neutral conditions, all PFOS molecules ($pK_a = -3.27$) are also dissociated to anionic form and are negatively charged, as is the surface of the virgin PMIA membrane. The filtration of PFOS is affected by two factors: first, the electrostatic repulsion between negative charges on the membrane surface and negative charges of the ionized PFOS molecules; and second, the electrostatic attraction between the positive charges of the ammonium ions of OMMT molecules and the negative charges on ionized PFOS molecules. After saturation of the membrane surface by solutes, the rejection of PFOS molecules reaches a constant value and does not change over time. The enhancement in OMMT concentration increases the obstructive properties, attributed to the chemically bonded silicate layers with high aspect ratios, which efficiently hinder the diffusion of PFOS molecules into the nanocomposite membranes (Van de Witte et al., 1996). According to SEM images (Fig. 5b), by increasing the concentration of OMMT, membranes are formed with denser and thinner skin layers, higher porosity, and higher hydrophilicity (Fig. 4). Membranes with these characteristics give higher permeation. It can be found in Fig. 5b that the permeation is decreased when the OMMT concentration in the casting solution is higher than 4 wt.%, so we conducted follow-up experiments at concentrations under 4 wt.%. Furthermore, the thickness of the skin layer and the structures of the surface and sub-layer change, causing a decrease in the permeability of the nanocomposite membrane. Comparison of the results of the commercial and fabricated membranes revealed that the performance (permeation and rejection) of the commercial membrane was lower compared to the nanocomposite membranes.

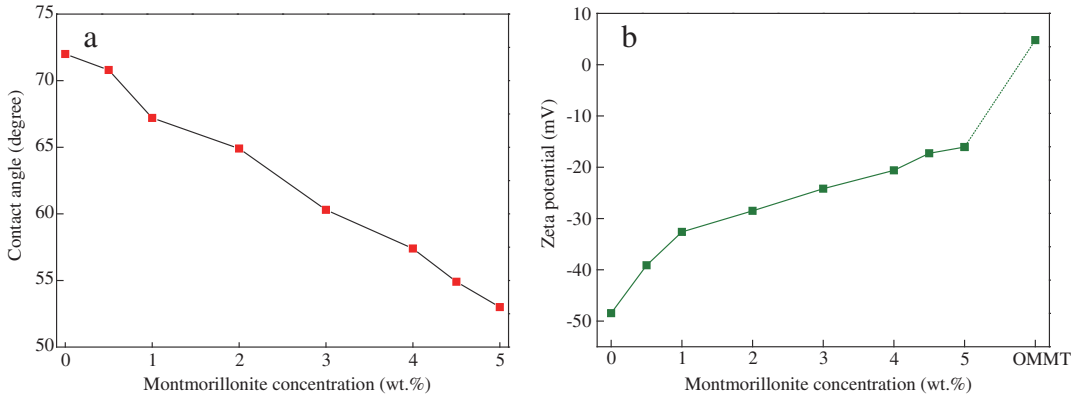

Fig. 4 – Water contact angles (a) and zeta potentials (b) of pristine PMIA and nanocomposite membranes prepared with various concentrations of OMMT. PMIA: poly(*m*-phenylene isophthalamide); OMMT: organically modified montmorillonite.

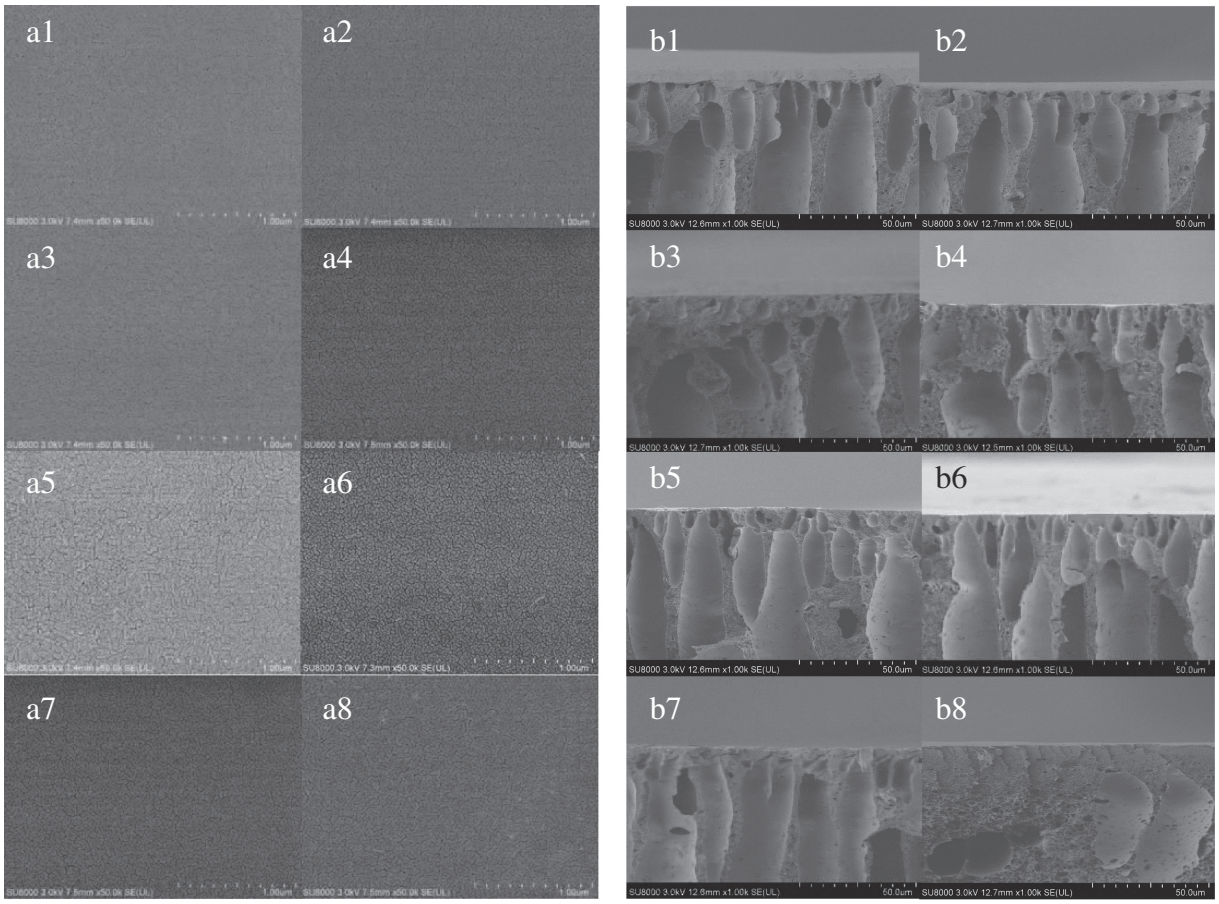

Fig. 5 – (a) SEM and (b) cross section SEM images of surface textures of membranes. (1) pristine PMIA; (2) PMIA/OMMT$_{0.5}$; (3) PMIA/OMMT$_{1.0}$; (4) PMIA/OMMT$_{2.0}$; (5) PMIA/OMMT$_{3.0}$; (6) PMIA/OMMT$_{4.0}$; (7) PMIA/OMMT$_{4.5}$; (8) PMIA/OMMT$_{5.0}$. Blue line: flux; red line: rejecting of PFOS.

2.4. *Effect of PFOS concentration on the performance of nanocomposite membranes in removal of PFOS*

The rejection and permeation results for the solution containing different PFOS concentrations, using a nanocomposite membrane with 4 wt.% concentration of OMMT in neutral conditions (pH 7.0), are depicted in Fig. 7. PFOS rejection increased with increasing PFOS concentration at all trans-membrane pressures. This is because as the initial concentration of PFOS in water was increased, more PFOS molecules were adsorbed on the membrane surface, causing the pore size of the membranes to decrease, and strengthening the screening effect of the membrane surface, resulting in the enhancement of rejection.

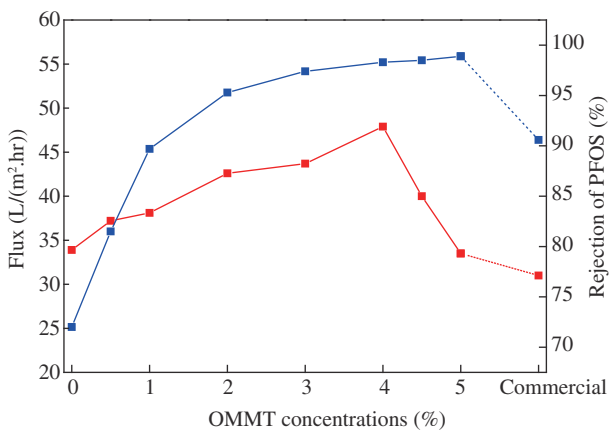

Fig. 6 – Effect of OMMT concentration on the rejection and permeation of solution containing PFOS. OMMT: organically modified montmorillonite; PFOS: perfluorooctane sulfonate.

2.5. *Effect of co-existing anions on the performance of nanocomposite membranes in removal of PFOS*

The effect of co-existing anions is an important factor in evaluating the applicability of OMMT nanofiltration membranes in PFOS removal. Many anions, such as chloride (Cl^-), sulfate (SO_4^{2-}), and phosphate (PO_4^{3-}), are commonly found in the hydrosphere, which may compete with PFOS on the surface of the membranes. The effects of these anions on PFOS removal with three different concentrations (0, 0.01, and 0.1 mmol/L) were examined, and the results are illustrated in Fig. 8. The operating pressure was 5.5×10^5 Pa (79.75 psi). The presence of phosphate (PO_4^{3-}) had the most significant effect on the removal of PFOS. This can be attributed to the increased electronegativity of the membrane surface, leading

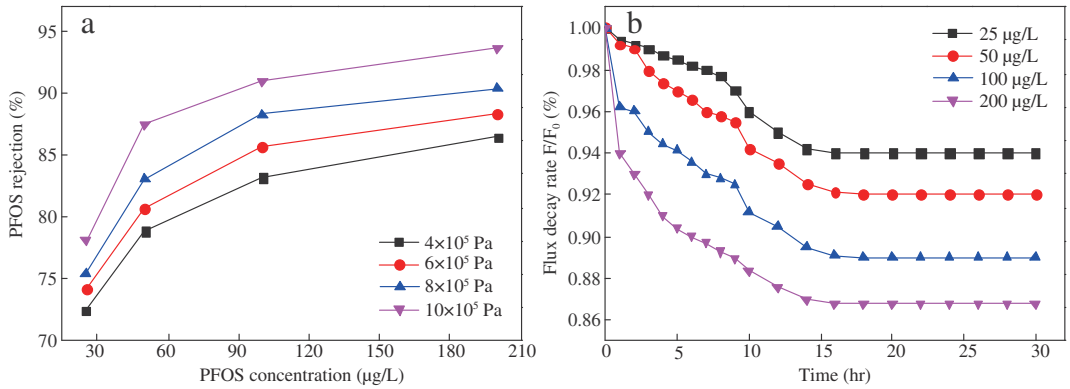

Fig. 7 – (a) Effect of PFOS concentration on the removal of PFOS and (b) flux decay rate F/F_0 in the presence of different PFOS concentrations: F is flux at a given time; F_0 is the pure water flux. PFOS: perfluorooctane sulfonate.

to enhanced electrostatic repulsion between the membrane surface and PFOS molecules. As we can see from Fig. 8, the zeta potentials of the composite membranes in the presence of various anionic additives were more negative, supporting the effect of co-existing anions on PFOS rejection.

2.6. Effect of Pb^{2+} on the performance of nanocomposite membranes in removal of PFOS

To study the effect of heavy metal ions on PFOS rejection, lead chloride ($PbCl_2$), which is typically present in water, was used to provide background electrolyte lead ions. As we can see from Fig. 9, the rejection of PFOS was increased with the enhancement in Pb^{2+} concentration at all trans-membrane pressures. The improvement can be attributed to the complexation between lead ions and PFOS molecules. We have previously found that bridging can occur between Ca^{2+} ions and the sulfonate functional groups in PFOS molecules, and we have quantified the calcium-bridging mechanism using DFT calculations (Zhao et al., 2013). Further interactions between Pb^{2+} ions and the sulfonate functional groups in PFOS molecules are still under study. The permeate flux decreases with increasing Pb^{2+} concentration in Fig. 9, indicating that more Pb^{2+} ions and sulfonate functional groups from PFOS molecules precipitated on the membrane surface, resulting in the pore blockage effect.

Fig. 10 shows two- and three-dimensional image profiles of AFM images of the surfaces of membranes. In these images, the brightest area represents the highest point on the membrane surface, and the dark regions indicate valleys or membrane pores. The surface morphologies of the membranes were strongly influenced by the solution chemistry. The surface roughness parameters of the membranes are presented in Table 1. The roughness parameters of the membranes were increased by co-existing lead ions.

3. Conclusions

Nanocomposite PMIA membranes were prepared by addition of different concentrations of OMMT to the casting solution and by a combination of solution dispersion and wet-phase inversion methods. The layered clay had a significant effect

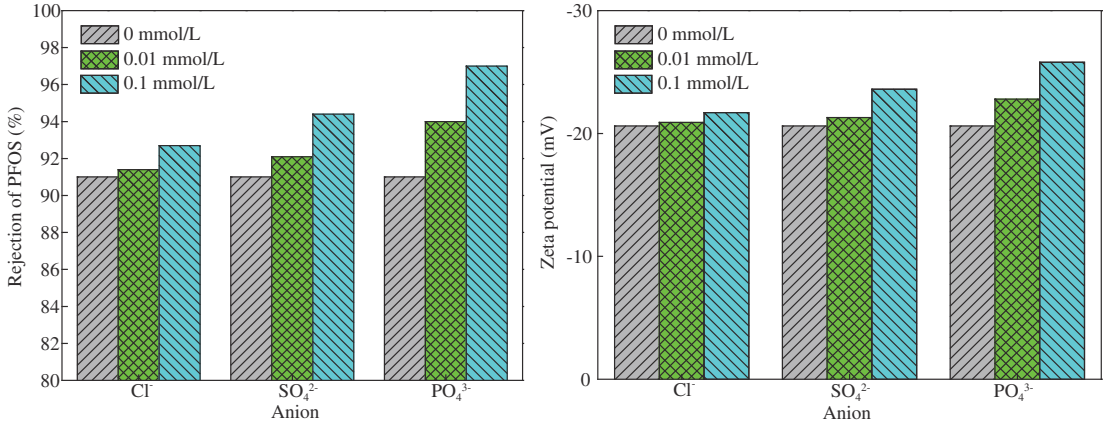

Fig. 8 – Effect of co-existing anion concentration on the removal of PFOS (a) and zeta potentials (b) of pristine PMIA and nanocomposite membranes. PFOS: perfluorooctane sulfonate; PMIA: poly(*m*-phenylene isophthalamide).

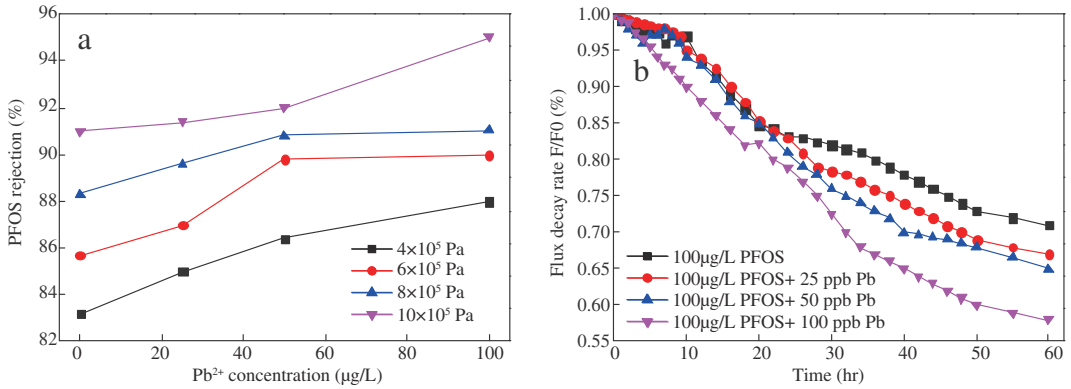

Fig. 9 – Effect of Pb^{2+} concentration on the removal of PFOS and flux decay rate F/F_0 at different Pb^{2+} concentrations. PFOS: perfluorooctane sulfonate.

on the membrane formation mechanism, which was investigated by SEM and AFM imaging. Addition of different concentrations of OMMT to the casting solution resulted in membranes with thinner skin layers. The data showed that the addition of OMMT can significantly improve membrane hydrophilicity and thermal resistance.

PFOS removal by the nanofiltration membranes was improved through the incorporation of clay mineral platelets into the PMIA membrane structure. The removal of PFOS by the fabricated membranes involved electrostatic repulsion between charged PFOS entities and similar charges on the membrane surface. The dominant mechanism in the removal of PFOS depended on the solute and membrane properties. Our results further reveal the remarkable potential of OMMT-modified nanofiltration membranes for contaminant removal applications in water treatment.

Acknowledgments

This work was financially supported by the National Natural Science Foundation of China (Nos. 21176245, 21476248), the National Science and Technology Support Program of China (Nos. 2012BAJ25B02, 2012BAJ25B06) and the special fund of the

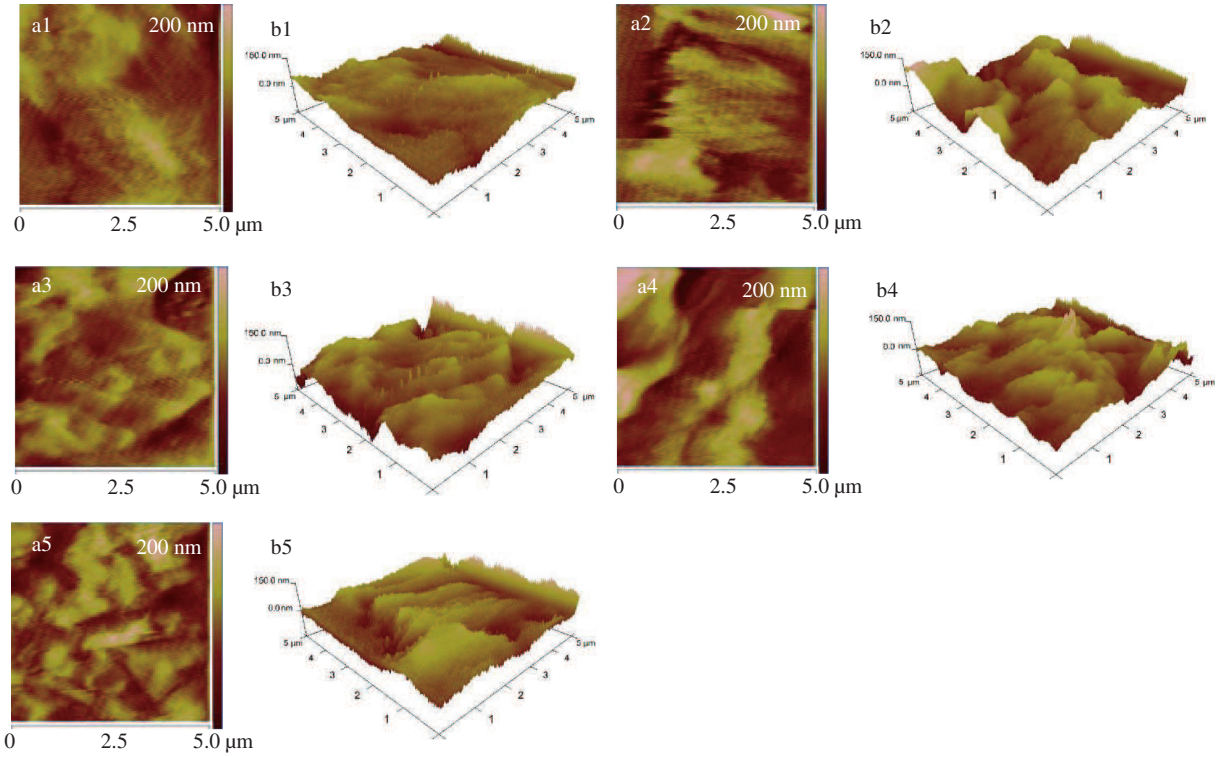

Fig. 10 – AFM images of (a) pristine PMIA/$OMMT_{4.0}$ membrane; (b) before and after filtration of 100 μg/L PFOS; (c) 100 μg/L PFOS and 25 μg/L Pb^{2+}; (d) 100 μg/L PFOS and 50 μg/L Pb^{2+}, (e) 100 μg/L PFOS and 100 μg/L Pb^{2+}. PFOS: perfluorooctane sulfonate; PMIA: poly(*m*-phenylene isophthalamide); OMMT: organically modified montmorillonite.

Table 1 – Roughness parameters and contact angles of prepared membranes, and PFOS accumulation on membrane surfaces in different experimental systems.

Feed system	R_a (nm)	R_q (nm)	R_{max} (nm)
Pristine PMIA/OMMT$_{4.0}$ membrane	22.5	28.6	164
100 μg/L PFOS	30.2	38.1	202
100 μg/L PFOS +25 μg/L Pb^{2+}	34.8	43.1	205
100 μg/L PFOS +50 μg/L Pb^{2+}	33.2	40.6	227
100 μg/L PFOS +100 μg/L Pb^{2+}	50.6	61.9	345.7

State Key Joint Laboratory of Environment Simulation and Pollution Control (No. 12L02ESPC).

REFERENCES

Anadão, P., Sato, L.F., Wiebeck, H., Valenzuela-Díaz, F.R., 2010. Montmorillonite as a component of polysulfone nanocomposite membranes. Appl. Clay Sci. 48 (1–2), 127–132.

Baker, R.W., 2004. Membrane technology and applications. second ed. John Wiley & Sons, England.

Chen, Z., Chen, F.L., Zeng, F.S., Li, J.M., 2014. Preparation and characterization of the charged PDMC/Al_2O_3 composite nanofiltration membrane. Desalination 349, 106–114.

Cheng, L.P., Lin, D.J., Yang, K.C., 2000. Formation of mica-intercalated-nylon 6 nanocomposite membranes by phase inversion method. J. Membr. Sci. 172 (1–2), 157–166.

Fang, Y.M., Duranceau, S.J., 2013. Study of the effect of nanoparticles and surface morphology on reverse osmosis and nanofiltration membrane productivity. Membranes 3 (3), 196–225.

Gevers, L.E.M., Vankelecom, I.F.J., Jacobs, P.A., 2005. Zeolite filled polydimethylsiloxane (PDMS) as an improved membrane for solvent-resistant nanofiltration (SRNF). Chem. Commun. 19, 2500–2502.

Gholami, A., Moghadassi, A.R., Hosseini, S.M., Shabani, S., Gholami, F., 2014. Preparation and characterization of polyvinyl chloride based nanocomposite nanofiltration-membrane modified by iron oxide nanoparticles for lead removal from water. J. Ind. Eng. Chem. 20 (4), 1517–1522.

Giesy, J.P., Kannan, K., 2001. Global distribution of perfluorooctane sulfonate in wildlife. Environ. Sci. Technol. 35 (7), 1339–1342.

Kimura, K., Amy, G., Drewes, J., Watanabe, Y., 2003. Adsorption of hydrophobic compounds onto NF/RO membranes: an artifact leading to overestimation of rejection. J. Membr. Sci. 221 (1–2), 89–101.

Lu, H.D., Hu, Y., Ling, M., Chen, Z.Y., Fan, W.C., 2006. Structure characteristics and thermal properties of silane-grafted-polyethylene/clay nanocomposite prepared by reactive extrusion. Compos. Sci. Technol. 66 (15), 3035–3039.

Monticelli, O., Bottino, A., Scandale, I., Capannelli, G., Russo, S., 2007. Preparation and properties of polysulfone-clay composite membranes. J. Appl. Polym. Sci. 103 (6), 3637–3644.

Moody, C.A., Field, J.A., 2000. Perfluorinated surfactants and the environmental implications of their use in fire-fighting foams. Environ. Sci. Technol. 34 (18), 3864–3870.

Moody, C.A., Kwan, W.C., Martin, J.W., Muir, D.C.G., Mabury, S.A., 2001. Determination of perfluorinated surfactants in surface water samples by two independent analytical techniques: Liquid chromatography/tandem mass spectrometry and ^{19}F NMR. Anal. Chem. 73 (10), 2200–2206.

Namvar-Mahboub, M., Pakizeh, M., 2013. Development of a novel thin film composite membrane by interfacial polymerization on polyetherimide/modified SiO_2 support for organic solvent nanofiltration. Sep. Purific. Technol. 119, 35–45.

Nigam, V., Setua, D.K., Mathur, G.N., Kar, K.K., 2004. Epoxy-montmorillonite clay nanocomposites: Synthesis and characterization. J. Appl. Polym. Sci. 93 (5), 2201–2210.

Pages, N., Yaroshchuk, A., Gibert, O., Cortina, J.L., 2013. Rejection of trace ionic solutes in nanofiltration: Influence of aqueous phase composition. Chem. Eng. Sci. 104, 1107–1115.

Pourjafar, S., Rahimpour, A., Jahanshahi, M., 2012. Synthesis and characterization of PVA/PES thin film composite nanofiltration membrane modified with TiO_2 nanoparticles for better performance and surface properties. J. Ind. Eng. Chem. 18 (4), 1398–1405.

Rajesh, S., Ismail, A.F., Mohan, D.R., 2012. Structure–property interplay of poly (amide–imide) and TiO_2 nanoparticles impregnated poly (ether-sulfone) asymmetric nanofiltration membranes. RSC Adv. 2 (17), 6854–6870.

Rattanaoudom, R., Visvanathan, C., Boontanon, S.K., 2012. Removal of concentrated PFOS and PFOA in synthetic industrial wastewater by powder activated carbon and hydrotalcite. J. Water Sustain. 2 (4), 245–258.

Ren, X.J., Zhao, C.W., Du, S.S., Wang, T., Luan, Z.K., Wang, J., et al., 2010. Fabrication of asymmetric poly (*m*-phenylene isophthalamide) nanofiltration membrane for chromium (VI) removal. J. Environ. Sci. 22 (9), 1335–1341.

Romanos, G.E., Athanasekou, C.P., Katsaros, F.K., Kanellopoulos, N.K., Dionysiou, D.D., Likodimos, V., et al., 2012. Double-side active TiO_2-modified nanofiltration membranes in continuous flow photocatalytic reactors for effective water purification. J. Hazard. Mater. 211-212, 304–316.

Schafer, A.I., Fane, A.G., Waite, T.D., 2004. Nanofiltration: Principles and applications (hardbound). Elsevier Science, Oxford.

Schmidt, P., Bednarz, E.L., Lutze, P., Górak, A., 2014. Characterisation of organic solvent nanofiltration membranes in multi-component mixtures: Process design workflow for utilising targeted solvent modifications. Chem. Eng. Sci. 115, 115–126.

Tang, C.Y.Y., Fu, Q.S., Robertson, A.P., Criddle, C.S., Leckie, J.O., 2006. Use of reverse osmosis membranes to remove perfluorooctane sulfonate (PFOS) from semiconductor wastewater. Environ. Sci. Technol. 40 (23), 7343–7349.

Van de Witte, P., Dijkstra, P.J., Van den Berg, J.W.A., Feijen, J., 1996. Phase separation processes in polymer solutions in relation to membrane formation. J. Membr. Sci. 117 (1–2), 1–31.

Van der Bruggen, B., Schaep, J., Wilms, D., Vandecasteele, C., 1999. Influence of molecular size, polarity and charge on the retention of organic molecules by nanofiltration. J. Membr. Sci. 156 (1), 29–41.

Vecitis, C.D., Park, H., Cheng, J., Mader, B.T., Hoffmann, M.R., 2009. Treatment technologies for aqueous perfluorooctane sulfonate (PFOS) and perfluorooctanoate (PFOA). Front. Environ. Sci. Eng. China 3 (2), 129–151.

Wang, X.R., Si, Y., Wang, X.F., Yang, J.M., Ding, B., Chen, L., et al., 2013. Tuning hierarchically aligned structures for high-strength PMIA-MWCNT hybrid nanofibers. Nanoscale 5 (3), 886–889.

Yu, Y., Zhao, C.W., Wang, Y.G., Fan, W.H., Luan, Z.K., 2013. Effects of ion concentration and natural organic matter on arsenic(V) removal by nanofiltration under different transmembrane pressures. J. Environ. Sci. 25 (2), 302–307.

Zhai, Y.Y., Wang, N., Mao, X., Si, Y., Yu, J.Y., Al-Deyab, S.S., et al., 2014. Sandwich-structured PVdF/PMIA/PVdF nanofibrous separators with robust mechanical strength and thermal stability for lithium ion batteries. J. Mater. Chem. A 2 (35), 14511–14518.

Zhang, H.Q., Zhang, Y.J., Li, L.B., Zhao, S., Ni, H.O., Cao, S.K., et al., 2014. Cross-linked polyacrylonitrile/polyethyleneimine–polydimethylsiloxane composite membrane for solvent resistant nanofiltration. Chem. Eng. Sci. 106, 157–166.

Zhao, C.W., Zhang, J., He, G.Z., Wang, T., Hou, D.Y., Luan, Z.K., 2013. Perfluorooctane sulfonate removal by nanofiltration membrane the role of calcium ions. Chem. Eng. J. 233, 224–232.